HADAMARD TRANSFORM SEPERATION OF NTSC COMPONENT SIGNALS

J.Barba, N.Scheinberg, M.Colef, E.H.Feria

City College of New York
Department of Electrical Engineering
140 Street and Convent Ave.
New York, N.Y. 10031

ABSTRACT

The transmission of NTSC composite color images over digital communication channels is generally accomplished by coding the less correlated component signal, YIQ. Unless the video source is available, the component signals are separated from the composite signal by using comb-filters. Comb-filtering is generally performed in the temporal domain. This paper shows that by properly sampling the NTSC composite color signal at four times the color subcarrier, the Walsh-Hadamard transform acts like a comb filter and separates the YIQ components of the composite signal. The YIQ components will be mapped into specific locations of the coefficient matrix.

INTRODUCTION

In general if the arrray f(i,j) represents the samples of an NTSC composite image over an array of NxN points then the two-dimensional Walsh transform, F(u,v) and its inverse, are given by the matrix product:

$$[F(u,v)]=(1/N^2)[H(u,v)][f(i,j)][H(u,v)] \quad (1)$$

$$[f(i,j)]=[H(u,v)][F(u,v)][H(u,v)] \quad (2)$$

where [H(u,v)] is the Hadamard matrix consisting of Walsh functions of order N. The result of the Walsh transformation is a NxN coefficient matrix where each coefficient represents the projection of the data matrix onto a particular Walsh-Hadamard basis matrix pattern. Data compression can be achieved because the image energy which is usually uniformly distributed in the spatial domain, tends to be concentrated into those transform coefficients which represent the lower frequency components of the Walsh domain. The majority of the other transform coefficients are always nearly zero and need not be transmitted.

WALSH SPECTRUM

The energy distribution of a typical 8x8 coefficient matrix is shown in Fig.1 along with the location of the chrominance components.

The NTSC composite color signal is given by:

$$S(t)=Y(t)+I(t)\cos(2\pi f_{sc}t+33^{o})+ +Q(t)\sin(2\pi f_{sc}t+33^{o}) \quad (3)$$

The color signals appear as amplitude modulated waveforms where the amplitudes of the modulated waveform are the baseband color differential signals. The phase of the modulated waveforms always changes 180^{o} from line to line. When the sampling frequency is equal to four times the color subcarrier and the sampling occurs at 12^{o}, 102^{o}, 192^{o}, and 282^{o} of the color subcarrier, the sampled modulated I and Q signals will be as shown in Fig.2. Thus, if we consider an 8x8 data matrix in the two dimensional space, the patterns of the modulated signals, I and Q, will be the same as the pattern of the two dimensional Walsh-Hadamard basis matrix (7,4) and (7,3) respectively. To see this, consider the set of N^2 8x8 basis matrix shown in Fig.3. We notice that the sampled modulated signals Q and I shown in Fig.2 correspond exactly to the horizontal Walsh basis function of sequency 3 and 4 respectively. In the vertical direction the subcarrier phase changes 180^{o} from line to line which corresponds to the Walsh basis function of sequency 7.

CH2118-8/85/0000-1313 $1.00 © 1985 IEEE

Authorized licensed use limited to: Peking University. Downloaded on November 23,2025 at 14:10:07 UTC from IEEE Xplore. Restrictions apply.

In the above observations the baseband I and Q signals were assumed to be of constant amplitude. In reality the baseband I and Q signals will vary as a function of time. They will thus have their respective bandwidths in the Walsh domain. The result is that there are coefficients in the Walsh domain which represent the higher components of the I and Q signals as shown in Fig.1. To understand how the Q and I bandwidth for Fig.1 were obtained we must consider Fig.3. We notice that Wal(3,y) which corresponds to Q and Wal(4,y) which correspondsto I have the same frequency in the x direction but are phase shifted by 90^{o} with respect to each other. The higher frequency components of the Q and I signals must be projected onto basis matrix patterns which preserve this phase relationship. To see which terms in the coefficient matrix correspond to the higher frequency components of the chrominance signal consider Fig.4. In Fig.4-a we show the sign of the subcarrier samples when the sampling rate is $4f_{sc}$. Fig.4-b and Fig.4-d show the sign of possible rates of change in the horizontal direction for the baseband Q signal. Fig.4-c and Fig.4-e represent the sign of the resulting modulated Q signal. We notice that the modulated Q signal in Fig.4-c corresponds to the Walsh function of sequency 2. We can thus relate this result to our coefficient matrix by stating that the coefficient (7,2) will contain all the higher frequency components of Q since the corresponding basis matrix corresponds to frequency variations of up to 0.89 MHz. Notice that the modulated Q waveform shown in Fig.4-e corresponds to the Walsh function of sequency 1. This waveform corresponds to the coefficient (7,2) and need not be consider since it corresponds to frequency components between 0.89 and 1.79 MHz. An interesting point to notice is that although the coefficient (7,2) is lower in spatial frequency in the Walsh domain than the coefficient (7,3), it corresponds to a higher frequency component of the Q signal in the temporal domain. Similar arguments can be used to argue that the coefficient (7,5) will correspond to the higher frequency components of the I signal.

In the vertical direction the color variations in principle can change from line to line. However, this is generally not the case. The vertical variations in color will generally be similar to those in the horizontal direction.

The luminance signal, on the other hand, will in general not be mapped onto the Walsh basis matrix (7,4) and (7,3) and thus will not be mapped onto the coefficients in the Walsh domain which correspond to the I and Q signals. This is similar to what occurs in the Fourier domain where the luminance signal generally does not occupy the same frequency range as the chrominance signal.

If the sampling phase relative to the color subcarrier deviates from the above, the basis vectors (7,3) and (7,4) will no longer correspond to the vectors of the chrominance signals. The result will be that the coefficients (7,3) and (7,4) would now contain components of both the Q and I signals. Thus, if the Q and I signals are not to be separated then the sampling phase is unimportant. However the amount of compression is identical in both cases.

The above observations lead to the conclusion that if the NTSC composite signal is properly sampled at four times the color subcarrier, the Walsh-Hadamard transformation acts like a comb-filter which separates the YIQ components of the NTSC composite signal into specific locations of the coefficient matrix.

SIMULATION RESULTS

Five color images were used to simulate the component seperation of NTSC composite signals in the Hadamard domain. Four of the images are the standard test slides SMPTE1, SMPTE2, SMPTE3 and SMPTE15. The fifth image was that of a Boy playing with toys. The R,G,B signals of each image were sampled at four times the color subcarrier and stored in a VAX-750 computer. Linear combinations of RGB were used to generate the YIQ signals. The Q and I signals were bandlimited to 0.5MHz and 1.5MHz respectively, modulated by the subcarrier with the phase relation shown in Fig.2, and summed with the Y signal to generate the composite signal. The composite signals were used as the input to test the component separation of the Hadamard transform. A standard comb filter with vertical enhancement is also simulated for comparision.

The standard deviation was used to determine which transform coefficients to assign to each componet signal. The three signals $Y(t)$, $I(t)\cos(2\pi f_{sc}t+33^{o})$ and $Q(t)\sin(2\pi f_{sc}t+33^{o})$ were transformed separately for each of the five images. The standard deviation equals the positive square root of the variance given by:

Authorized licensed use limited to: Peking University. Downloaded on November 23,2025 at 14:10:07 UTC from IEEE Xplore. Restrictions apply.

$$\sigma_L^2(i,j) = \frac{1}{T}\left[\sum_{k=1}^{T} F_L^2(i,j) - \frac{1}{T}\left(\sum_{k=1}^{T} F_L(i,j)\right)^2\right] \quad (4)$$

$$i,j = 1,2,..,N$$

T = Total number of transform matrices

The standard deviation for the three signals $Y(t)$, $I(t)\cos(2\pi f_{sc} t + 33^\circ)$ and $Q(t)\sin(2\pi f_{sc} t + 33^\circ)$ averaged over the active video portion of the five images are given in Table I. A particular coefficient is assigned to the signal which has the largest standard deviation for the particular coefficient. The coefficient assignment for a 4x4, 8x8 and 16x16 transform are given in Table II.

The procedure to recover the baseband component signal from the Hadamard coefficients is given below:

1) Set to zero those coefficients which don't correspond to the particular signal being recovered.

2) In general, for an NxN transform of the modulated chrominance signals are related to the Hadamard transform of the baseband signal by :

$$F_{L_m} = \frac{1}{N^2} F_L(u \oplus (N-1), v \oplus k); L=Q \text{ or } I \quad (5)$$

$$k = \begin{cases} (N/2)-1 & ; L=Q \\ N/2 & ; L=I \end{cases}$$

where $\oplus$ = sum modulo 2 and arguments are expressed in binary.

If either of the chrominance signals is being recovered, multiply the coefficients by 2 and remap the coefficients by the inverse operation of Eq.5.

3) Perform the inverse Hadamard transform to obtain the recovered baseband signal.

The signal-to-noise ratio (SNR) of the recovered signal is given by:

$$SNR = -10 \log\left[\frac{\frac{1}{N}\sum_{k=1}^{N}(S_j - \hat{S}_j)^2}{255^2}\right] \quad (6)$$

where: $\hat{S}$ = Recovered baseband signal.
S = Original baseband signal.
N = Total number of samples in the image.

The resulting SNR obtained using the Hadamard transform are presented in Table III. For comparision, the results obtained with the one line delay comb filter with vertical enhancement (Fig.5) are also shown in Table III. From Table III we notice that the Hadamard transform performed better than the comb filter in all cases. The performance is especially noticable in the chrominance separation. We also notice that the component separation generally improves as the transform size increases. This results because as the window (which truncates the data) increases in size less high frequency energy is generated from convolving the signal and window spectrum.

CONCLUSION

This paper presented a technique by which the NTSC component signals can be separated in the Hadamard domain. The technique was compared to a one line delay comb filter with vertical enhancement and shown to perform better with the five test images used.

REFERENCES

1) "A Practical Charge-Coupled Device Filter For The Separation of Luminance and Chrominance Signals in a Television Receiver", Steve Barton, IEEE Trans. Consumer Elect., Vol. CE-23, No.3 August 1977.

2) "Some Thoughts on Using Comb Filters In The Broadcast Television Transmitter And at The Receiver", Rudolt Turner, IEEE Trans. Consumer Elect. Vol. CE-23, No.3 August 1977.

3) "Computer Image Processing And Recognition", Ernest L. Hall, Academic Press, 1979.

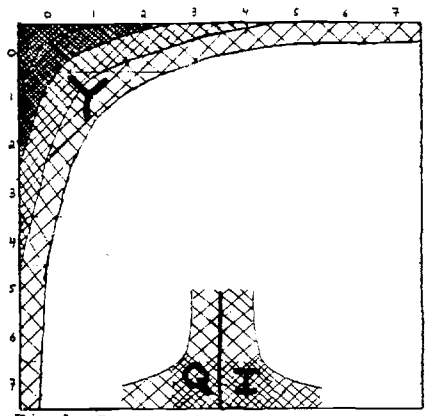

Fig.1 Energy Distribution in Walsh-Hadamard Domain.
(1,1)=Average Luminance.
(7,3)=Average Q.
(7,2),(6,3)=Higher Freq.Components of Q.
(7,4)=Average I
(7,5),(6,4)=Higher Freq.Components of I.

Authorized licensed use limited to: Peking University. Downloaded on November 23,2025 at 14:10:07 UTC from IEEE Xplore. Restrictions apply.

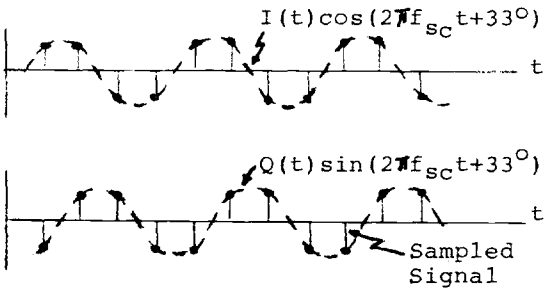

Fig.2 Phase Relationship Between the Sampling Clock and the Modulated I and Q Components.

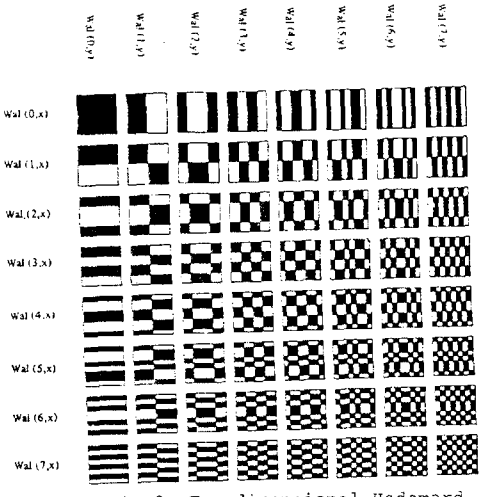

Fig.3 Two-dimensional Hadamard Basis Matrices. Black=1, White=-1.

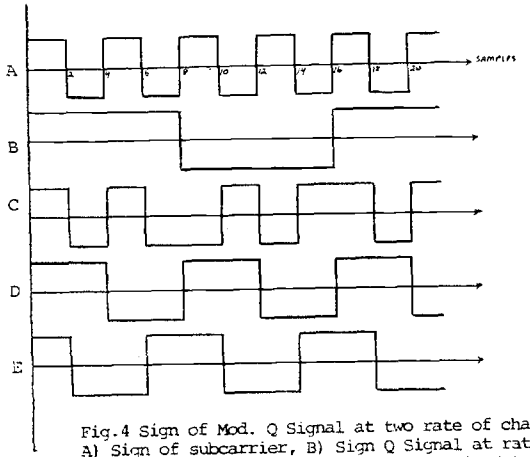

Fig.4 Sign of Mod. Q Signal at two rate of change. A) Sign of subcarrier, B) Sign Q Signal at rate of change= $f_{SC}/4$. C) Sign of Mod Q signal in (B). D) Sign of Q signal at rate of change=$f_{SC}/2$. E) Sign of Mod. Q signal in (D).

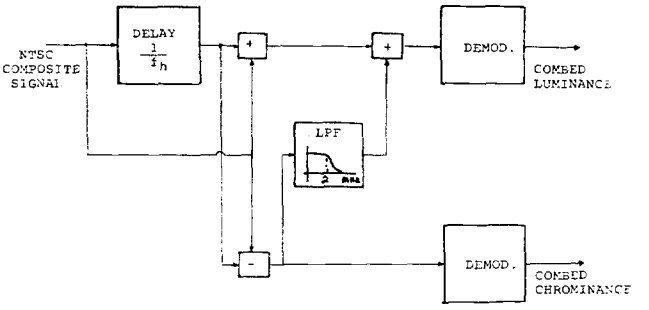

Fig.5 One Line Delay Comb Filter With Vertical Enhancement.

34.365	5.239	2.379	2.399	0.705	0.866	1.083	1.226
8.672	3.954	1.554	1.351	0.589	0.657	0.733	0.668
5.012	2.132	1.226	1.001	0.517	0.565	0.590	0.500
4.295	1.745	1.009	0.823	0.451	0.496	0.497	0.426
2.353	1.238	0.795	0.663	0.427	0.425	0.414	0.351
2.334	1.130	0.731	0.603	0.417	0.419	0.402	0.339
2.277	1.024	0.641	0.558	0.401	0.383	0.369	0.324
1.908	0.735	0.490	0.471	0.429	0.344	0.323	0.290

(a)

0.047	0.046	0.053	0.044	0.487	0.186	0.109	0.080
0.035	0.049	0.058	0.050	0.517	0.214	0.118	0.092
0.035	0.051	0.061	0.051	0.504	0.228	0.126	0.096
0.037	0.052	0.064	0.054	0.518	0.243	0.132	0.101
0.038	0.057	0.073	0.068	1.009	0.309	0.153	0.132
0.042	0.062	0.083	0.078	1.045	0.363	0.176	0.156
0.047	0.069	0.101	0.111	1.920	0.508	0.216	0.223
0.062	0.097	0.143	0.230	8.810	1.026	0.306	0.463

(b)

0.048	0.042	0.087	0.260	0.032	0.030	0.030	0.033
0.055	0.046	0.105	0.306	0.034	0.031	0.030	0.031
0.057	0.049	0.112	0.341	0.035	0.032	0.030	0.031
0.063	0.051	0.126	0.373	0.037	0.033	0.031	0.031
0.075	0.057	0.151	0.507	0.042	0.035	0.032	0.032
0.080	0.064	0.166	0.555	0.045	0.037	0.032	0.032
0.091	0.073	0.190	0.766	0.050	0.041	0.033	0.033
0.154	0.091	0.322	2.775	0.079	0.049	0.036	0.035

(c)

TABLE I
Standard deviation of 8x8 Hadamard transform coefficients of NTSC component signals averaged of 5 images.
a) Y signal b) mod. I signal c) mod. Q signal

	Q	I	Y
4x4	(4,2)	(4,3),(3,3)	All other
8x8	(8,3),(8,4),(7,4) (6,4)	(8,5),(8,6),(8,7) (8,8),(7,5),(7,6) (6,5),(6,6)	All other
16x16	(16,7),(16,8),(15,7) (15,8),(14,8),(13,8) (12,8),(11,8),(10,8) (9,8)	(16,9),(16,10),(16,11) (16,12),(15,9),(15,10) (15,11),(15,12),(14,9) (14,10),(14,11),(14,12 (13,9),(13,10),(12,9) (12,10),(11,9),(11,10) (10,9),(10,10),(9,9) (9,10),(8,9),(7,9) (6,9),(5,9),(4,9)	All other

TABLE II
Coefficient assignment to component signals

		SMPTE1	SMPTE2	SMPTE3	SMPTE15	BOY
COMB FILT	Y	38.25	38.81	38.19	39.79	37.67
	I	31.83	34.48	33.33	34.29	32.04
	Q	32.08	35.01	33.79	34.31	32.58
4x4 TRANS	Y	40.54	39.84	40.80	41.95	39.13
	I	40.22	39.38	40.02	41.82	38.06
	Q	41.27	39.90	41.75	42.62	39.87
8x8 TRANS	Y	41.37	40.03	41.53	42.73	39.57
	I	40.62	39.53	40.30	42.08	38.51
	Q	42.76	40.17	43.17	43.95	40.22
16x16 TRANS	Y	41.26	40.63	41.62	42.38	39.57
	I	42.99	39.77	39.95	41.68	38.60
	Q	42.99	41.17	43.19	43.88	41.36

TABLE III SNR in db.

Authorized licensed use limited to: Peking University. Downloaded on November 23,2025 at 14:10:07 UTC from IEEE Xplore. Restrictions apply.